Transactions of the 17th International Conference on Structural Mechanics in Reactor Technology (SMiRT 17)
Prague, Czech Republic, August 17 –22, 2003

Paper # C04-2

Studies on the Stress-strain State of Spacer Grids and Claddings

Igor Matsegorin, Alexander Semenov, Denis Severinov, Eugeny Rivkin, Anatoliy Kupalov-Yaropolk

Research and Development Institute of Power Engineering, Russia

ABSTRACT

This paper discusses the general principles of a procedure for investigating the distribution of residual and structural stresses in fuel assembly components. It also deals with the main findings of studies on distribution of residual stresses in fuel claddings and individual cells of spacer grids, which arise during manufacture, as well as with the results of studies on structural stresses which appear in the spacer grid after installation of all fuel rods.

The complete stress pattern was reconstructed by investigations on residual stress distribution across the fuel cladding wall. It was established that some finishing treatments resulted in nonuniform distribution of residual stresses in outer surface layers of fuel claddings.

Studies on spacer grids revealed the distribution of residual stresses caused by spacer grid manufacture as well as the distribution of operating structural stresses arising when fuel assemblies are put together.

An improved procedure and special devices provide express assessment of yield tensor components in difficult-of-access areas of intricately shaped industrial products.

Use of computers in research allows determining stress components with an error of 10 to 20 MPa.

KEY WORDS: fuel cladding, spacer grid, residual stresses, X-ray stress measurement, modelling, zirconium alloys

INTRODUCTION

In-service behaviour of reactor core components, such as claddings, pressure tubes, spacer grids and welded joints, is largely determined by the residual stresses arising in these components in the process of their manufacture. These stresses in highly anisotropic materials, such as zirconium alloys, are difficult to determine by calculations. In view of this, an experimental procedure has been developed, which is based on X-ray diffractometry and allows studying the distribution of stresses and texture in claddings with a ribbed or profiled surface as well as in difficult-of-access areas of spacer grids, nipples and welded buttons. It is possible to measure stresses in spacer grid cells – both empty and with fuel assemblies installed, including weld areas.

IMPROVED X-RAY PROCEDURE FOR STRESS MEASUREMENT

X-ray studies of stress distribution in fuel claddings and spacer grid cells, using a diffractometer DART-UM1, were performed on a specially designed goniometric attachment for target X-raying with precise positioning and orientation of specimens with curved surfaces. The specimen stresses were measured according to an improved X-ray diffraction procedure by the "$Sin^2\Psi$" method involving 6 to 12 rotation angles, with the angles chosen from the series (Ψ: 0°, 13°, 18°, 23°, 27°, 30°, 33°, 36°, 39°, 42°, 45°, 48°) for each local area of the specimen. To confine X-raying to specified areas of a specimen with a highly curved surface, e.g. to spacer grid indent areas, the collimated beam cross-section was reduced to 0.5 x 0.5 mm^2.

Optimal radiation of the X-ray tube anode and the interval of precision angles for diffractive reflections were selected for zirconium alloy E-110 (Table 1). For X-ray diffraction study of spacer grid cells made of zirconium-based alloys (alloy E-110), an X-ray tube with a Cr- Ka anode was selected to record the diffractive profile from the crystallographic plane (10.4) found in the precision area of angles $2\theta \subset (155 – 161)$ deg.

Statistical treatment of primary measurements and stress analysis proceeded on line with automatic X-ray diffraction scan by the "STRESS" program (Fig. 1).The exact position of the diffraction profile for each angle turn ψ of an examined specimen was calculated by locating the centre of gravity and the exact position of the profile maximum with parabolic approximation by the least-squares method, preceded by fluctuation smoothing.

Choice of radiation and diffractive reflections
for determining stresses in zirconium-based alloys by X-ray diffraction

Table 1

Radiation			Diffractive reflection			h, μm, (75%)	
Anode	Spectrum	λ, nm	(h k . l)	d, nm	2θ, deg.	ψ=0°	ψ=45°
Cr	K_α	0.229092	(10.4)ω,T	0.11691	156.93	4.4	3.0
	K_β	0.208480	(20.3)A,T (21.0) ω	0.10843 0.10576	148.06 160.55		
Fe	K_α	0.193728	(11.4)A,T	0.10065	148.47	5	4
	K_β	0.175653	(21.3)β,AT	0.090029	154.6		
Co	K_α	0.179021	(30.0) A	0.093271	147.35	8.2	5.3
	K_β	0.162075	(20.5)	0.082915	155.57		
Cu	K_α	0.154184	(22.0) A	0.080775	145.26	12	8.4
	K_β	0.139217	(10.7) T	0.071114	156.38		

The parameters of crystallographic lattice for αZr: a = 0.3231 nm; b = 0.5147 nm.
A, T – axial and tangential directions, respectively.

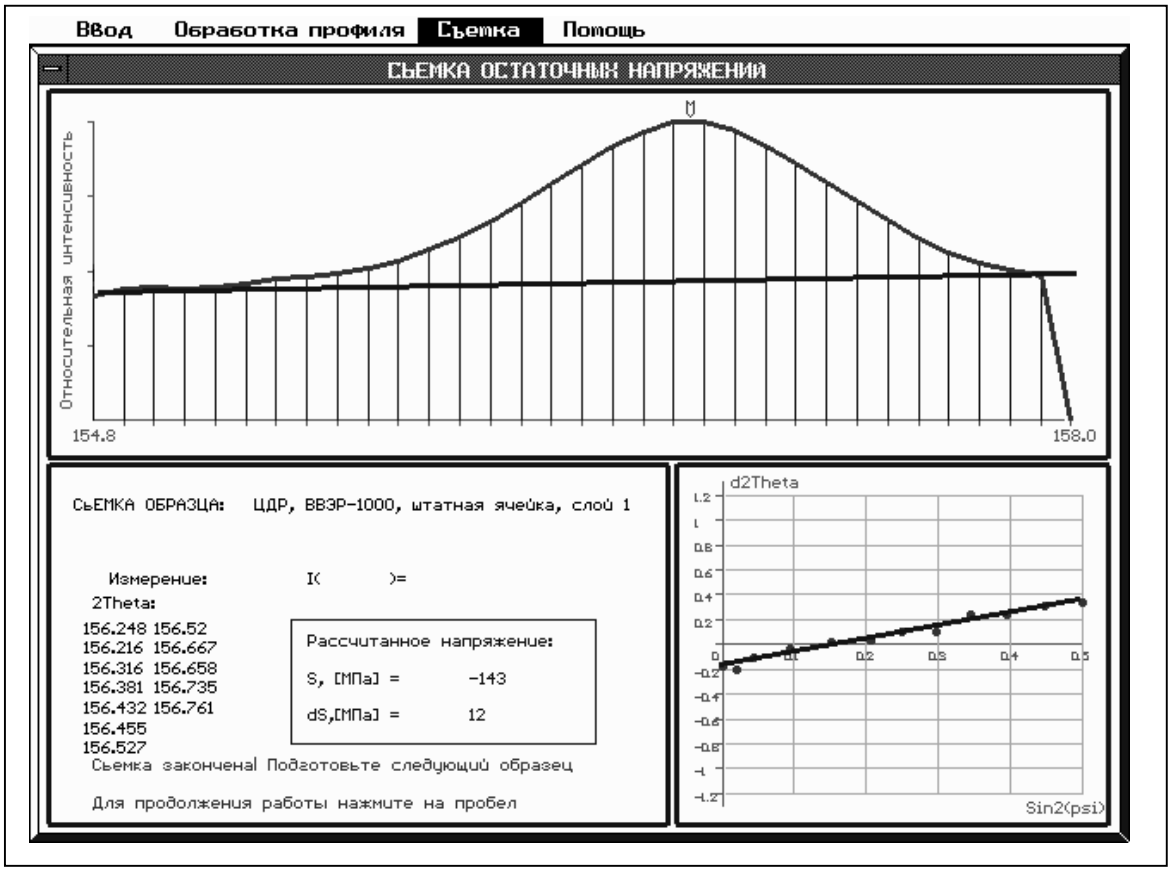

Fig. 1. Basic X-ray diffraction survey and stress analysis by the “STRESS” program.

Correction for defocusing of the setup geometry was made by repeating the survey and calculation for a reference specimen having the same surface curvature but being free from residual stresses.

Table 1 presents the recommended diffractive reflections for X-ray diffraction employed in measuring stresses in products made of zirconium-niobium alloys. The diffractive reflection column (hk.l) shows, besides, the possible superposition of phase lines and the recommended directions of measuring the stress component with the account for

the product texture.

To make sure that stresses in anisotropic materials are properly calculated, elastic module and Poisson ratios [1-3] were determined for the main directions in textured zirconium alloy products (see Table 2).

Elastic module and Poisson ratios for industrial components made of zirconium alloys

Table 2

Product	*Elastic modulus, GPa*			*Poisson ratio*		
	Ea	**Et**	**Er**	**νa**	**νt**	**νr**
E-110, cladding, spacer grid	97.6	96.2	102.4	0.32	0.33	0.33
E-635, cladding, spacer grid	99.3	97.6	100.5	0.32	0.33	0.33
125, pressure tube	97.4	99.5	98	0.32	0.33	0.33
E-125, pressure tube	97	99	100	0.32	0.33	0.33
CPS	97	98.5	99	0.32	0.33	0.33

where indices stand for: **a** – axial, **t** – tangential, and **r** – radial directions in a specimen.

The improved procedure under discussion was applied in investigating the distribution of residual stresses in fuel claddings and individual spacer grid cells as well as the structural stresses in components of a full-scale spacer grid.

STRESS DISTRIBUTION IN THE FUEL CLADDING

With the aim of streamlining the manufacturing process and improving the quality of fuel rods, an X-ray stress measurement study was carried out, involving fuel claddings with diameter Ø9×0.7 mm, made of E-110 zirconium alloy. The study revealed a complicated pattern of residual stress distribution across the wall of the tubular claddings. The surface layer of the claddings (Fig. 2) exhibited both tensile and compressive residual stresses reaching the extreme values of ±140 MPa and falling abruptly as the surface layer is removed by etching.

Analysis of the results suggests that the observed distribution of residual stresses in zirconium claddings was a combined effect of mechanical treatments at the final stage of their manufacturing cycle, such as tube straightening and final polishing. The straightening operation tends to set up mostly tensile stress near the surface layer, whereas polishing results in significant compressive stresses in the outer surface layer. The observed nodal distribution of alternating-sign stresses in a cladding with a low level of residual stresses suggests that the final etching of the outer surface of the cladding was irregularity and insufficiently deep.

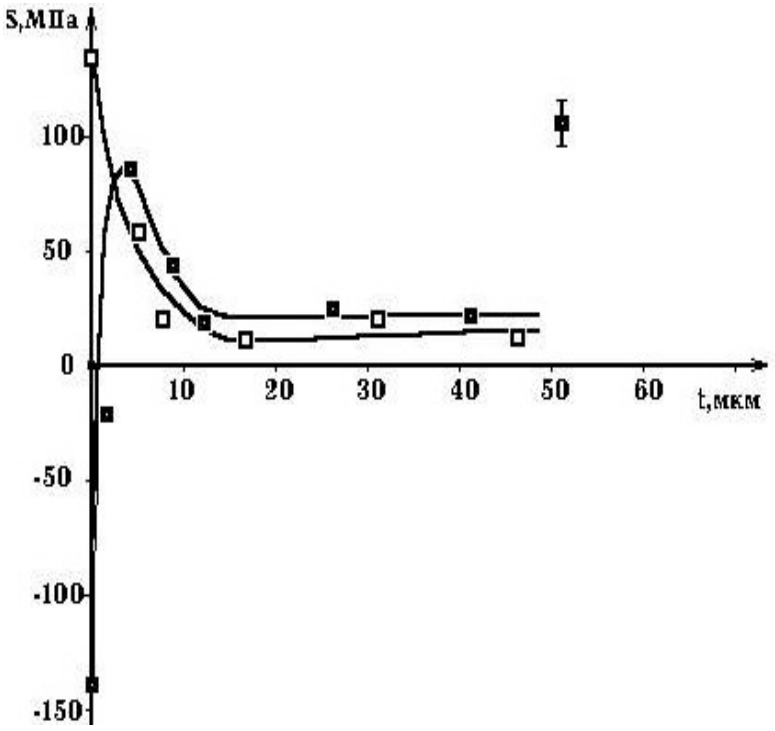

Fig. 2. Residual stress distribution across the cladding wall

STRESS DISTRIBUTION IN INDIVIDUAL SPACER GRID CELLS

The distribution of residual stresses across the wall thickness (up to six layers) was studied for individual spacer grid cells, made of E-110 alloy, at the sites of their possible concentration, such as indents and flexures. The measurements pointed to the absence of residual stresses in the cylindrical billets meant for fabrication of cells. Some cells showed a complicated pattern of residual stress distribution both round the section and across the wall thickness. Residual compressive hoop stresses were discovered in the indent areas, which had extreme values – up to (-180 MPa) – on the outer surface of the cell and relaxed as etching went down to 20-40 μm. In the prominent and bending areas of the section, residual tensile stresses were found to reach +100 MPa and +140 MPa, respectively, which also relaxed across the walls thickness.

Residual stress distribution was studied in five characteristic areas of spacer grid cells, made of E-110 alloy, with reconstruction of the true stress pattern across the cell wall. The measured residual stress distribution in as-manufactured cells had generally a bell-shaped pattern, with the extremes found at –450 MPa and +150 MPa. In spacer grid cells subjected to vacuum annealing at 580ºC for three hours, maximum residual stresses were no greater than 100 MPa in magnitude, as shown by all the samples investigated.

Studies were performed on distribution of stresses in cells caused by interference fit of fuel rods, whose dimensions were kept within the permissible range identified in the specifications. As the model cell expanded with the strain of pull increase from 50 μm to 150 μm, the tensile stresses showed practically monotonic variation from (+170 ± 15) MPa in area 1 (indent) to the peak of (+270 ± 20) MPa in area 4 (upper edge of the indent). Area 2 (convex flexure of the cell) was found under compressive stresses which showed almost linear variation up to (-160± 15) MPa, whereas in area 6 (flexure) stresses varied little, never exceeding 60 MPa in magnitude, i.e. the loading due to cell expansion caused by interference fit was "relaxed" by welded joints and was not be imparted to the flexure area. In other examined areas (3, 5, 6), variation of residual stresses due to interference fit was non-monotonic.

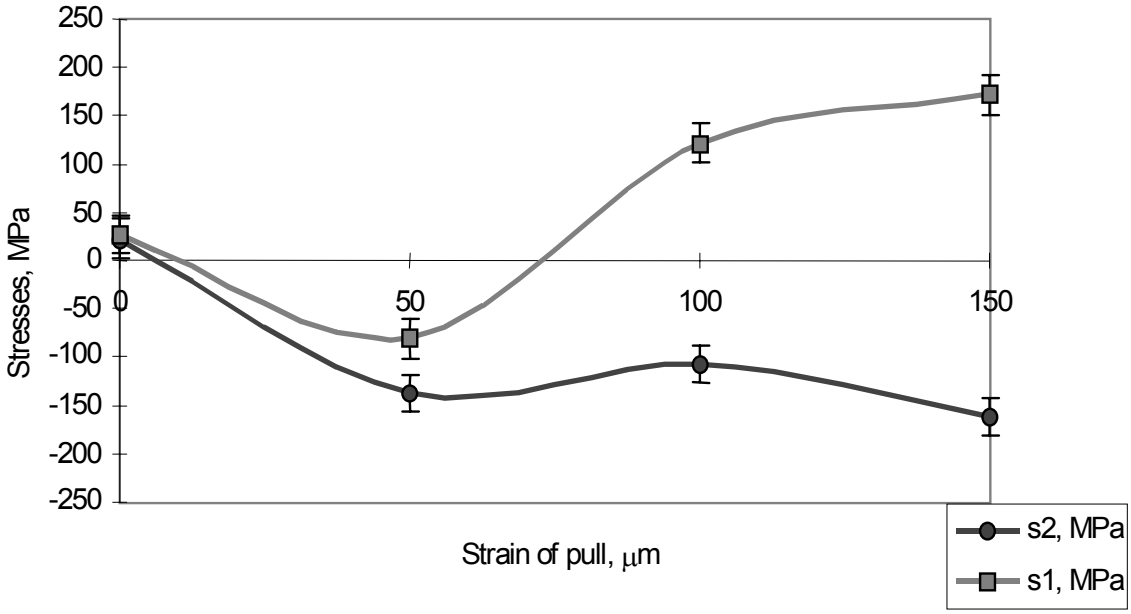

Figure 3
S1 – Linear (flat) area of spacer grid cell; S2 – flexure in the indent area;

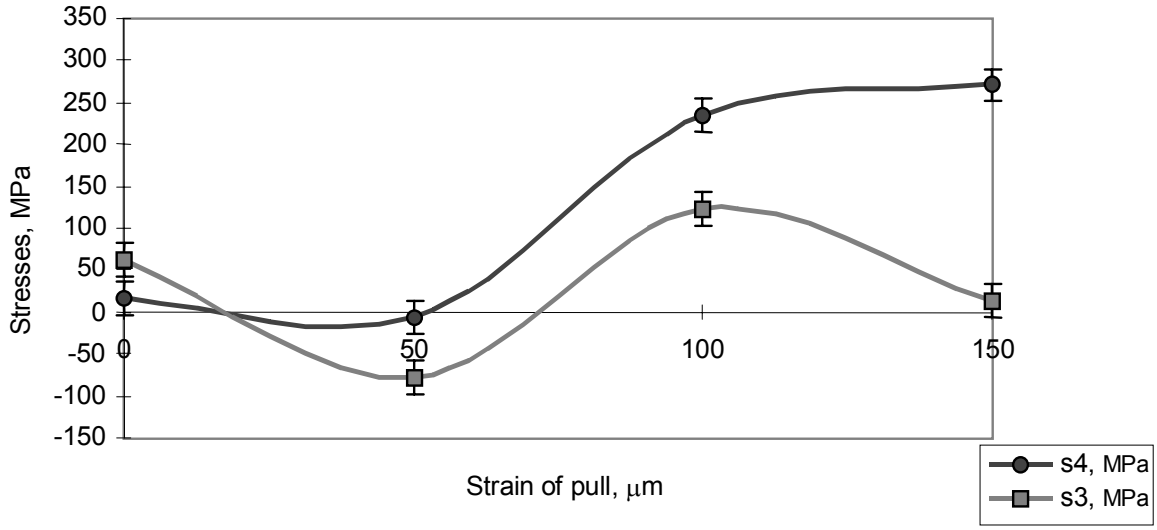

Figure 4
S3 – intermediate area of the cell indent; S4 – indent middle.

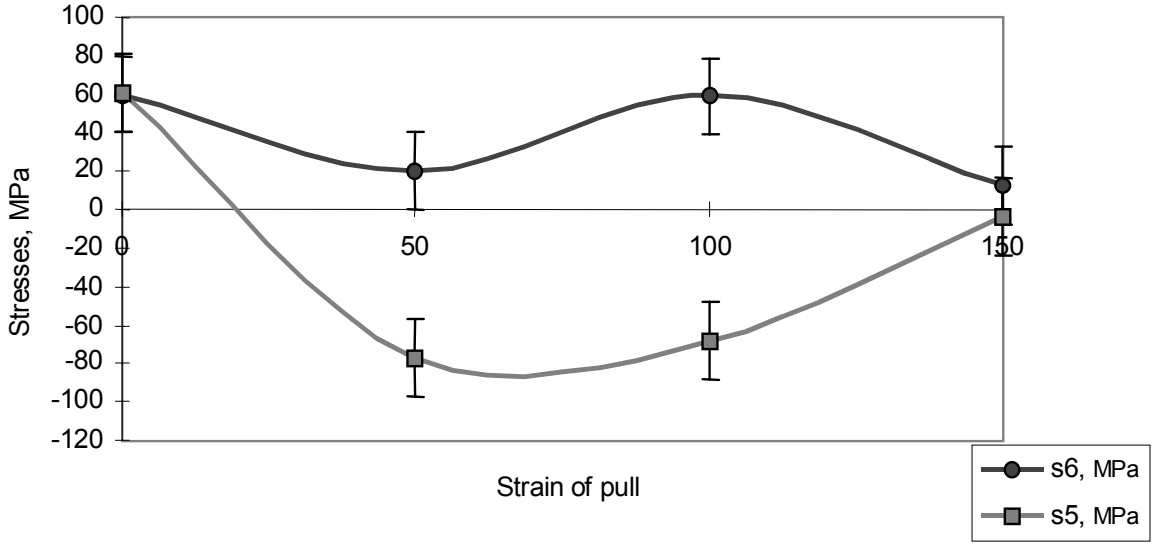

Figure 5
S5 – cell flexure; S6 – upper edge of the indent in longitudinal direction

STRESS DISTRIBUTION IN THE SPACER GRID

The spacer grid is one of the key components in the fuel assembly of a nuclear power reactor. Its sophisticated design and rigorous operating conditions, together with the importance of this component from the viewpoint of serviceability of the fuel assembly as a whole, impose high requirements on the spacer grid reliability and, hence, on its assessment methods. However, provision of a computer model for such a complicated component, with adequate response to the loads applied, and modelling of its behaviour in contact areas and at welds necessitate empirical information on the variation of real spacer grid condition under loading in order to make appropriate assumptions for calculations.

Distribution of hoop stresses on the inner surface of spacer grid cells, made of E-110 alloy, was studied with the use of the method described above. In order to rule out the effect of structural stresses resulting from manufacture on the stressed state of the spacer grid after fuel bundle formation, the specimen was subjected to final vacuum annealing at 580˚C for three hours. The following spacer grid cells were selected for the study: No. 1 – peripheral cell and No. 2 – intermediate cell (Fig. 6). The internal surfaces of both cells were bright-etched. The spacer grid was loaded by filling all its cells (except for the one investigated) with cylindrical empty fuel rods of hard brass with their diameters equal to the average nominal fuel rod diameter. The study proceeded in two stages, with the distribution of hoop stresses first studied in the peripheral cell and then in the intermediate cell. Besides, similar studies were staged with additional spacer grid loading by concentrated force P = 50 N, acting on the fixture near the indent in the radial direction (see Fig. 6).

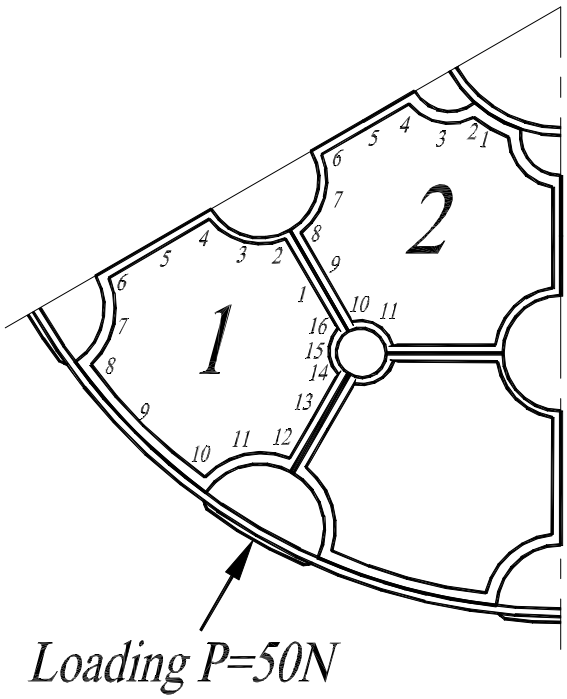

Fig. 6.

Local areas marked on the internal surface of the peripheral cell (No.1) and intermediate cell (No. 2).

On the internal surface of the cells, reference points were marked in characteristic areas, as shown in Fig. 6, in five cell layers equidistant in height (3 mm). Sixteen characteristic areas (80 points) were marked in cell No. 1 and 11 characteristic areas (55 points), in cell No. 2. In the absence of external loading, all the studied layers in peripheral cell No.1 showed cyclic stress distribution in the characteristic areas (Fig. 7). In flat areas (No. 1, 5, 9, 13), compressive stresses were discovered, typical of all the studied layers. Minor tensile stresses, typical of all the studied layers, were found near indents (areas No. 3, 7, 11, 15) – see Fig. 7. Indent areas (No. 3, 7, 11, 15) accounted for the humps and flat areas (No. 1, 5, 9, 13) for the dips in the stress distributions obtained, i.e. they were the sites of the extreme stress values.

The stresses measured in the other cell areas had intermediate values. The range of stress variations was observed to decrease with a certain positive trend in going from area No. 1 to area No. 16 (Fig. 7).

The average stress measurement error was 20 MPa (with 85 % confidence probability of the values). The averaged stress values calculated for all characteristic areas of each layer were practically equal to zero within the limits of measurement error. The maximum measured stresses were no higher than 50 MPa while the minimum stresses had a limit of –80 MPa. The stress range – the difference between the maximum and minimum stresses – changed little with layers, making 80 to 120 MPa, or 100 MPa on the average.

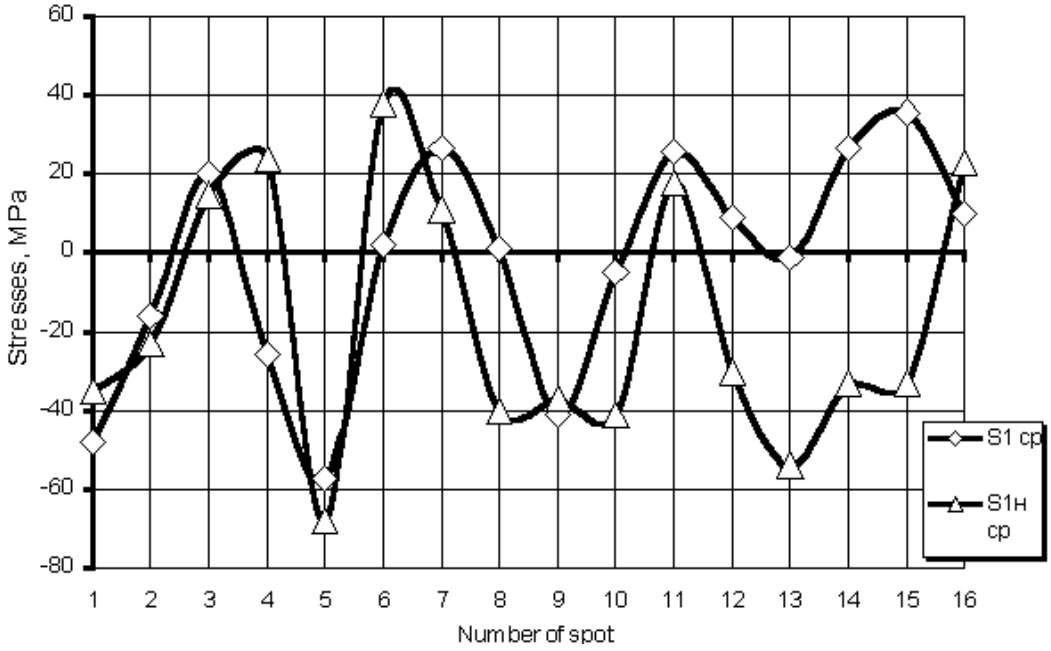

Figure 7
S1cp – height-averaged stresses in cell No. 1 without external loading
$S1_{н}$cp – height-averaged stresses in cell No. 1 with external loading

Study of peripheral cell No. 1 under external loading of P=50 N applied to the spacer grid, showed a certain deviation from the cyclic distribution of stresses, observed under no-load conditions, in the characteristic areas of each layer. This difference becomes clear when the layer-averaged stresses prior to loading, S1cp, and afterwards, $S1_{Н}$cp , are compared (Fig. 7).

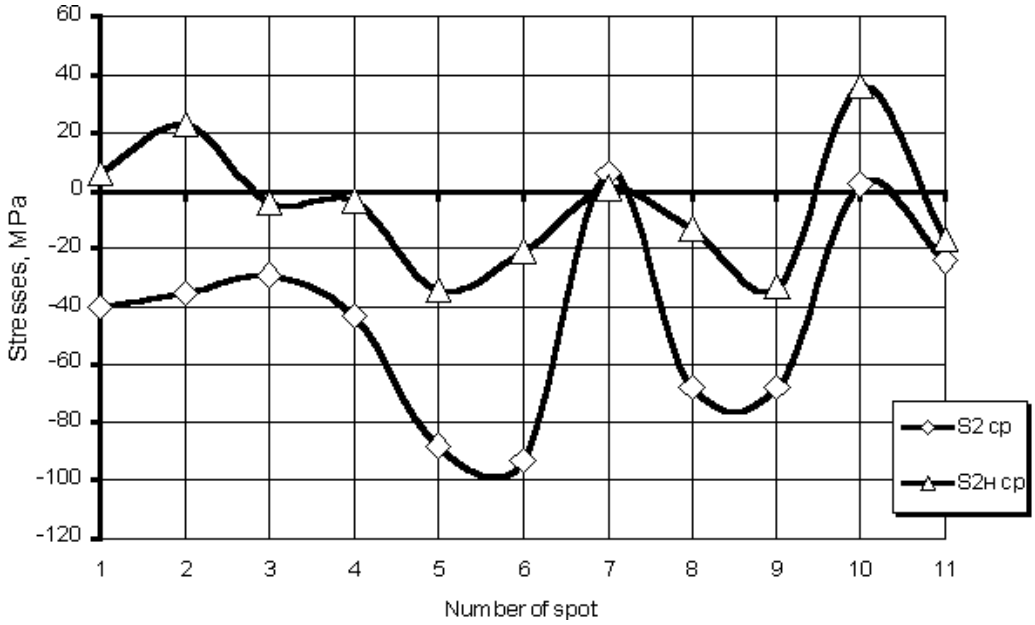

Figure 8
S2cp – height-averaged stresses in cell No. 2 without external loading
$S2_{н}$cp – height-averaged stresses in cell No. 2 with external loading

Comparison of the distributions shows all the flexures to be affected, except for those “farthest” from the load action line (areas No. 2, 16). On the other hand, areas No. 1, 5, 9 are seen to be unaffected, while area No. 13 –

previously uninvolved – shows perceptible effects of loading. With the indents, stress variation is only observed in area No. 15.

Studies on intermediate cell No. 2, free from external loading, also came up with a cyclic pattern of stress distribution in characteristic areas of each layer (Fig. 8).

Compressive stresses, typical of all the examined layers, were discovered in flat areas (No. 1, 5, 9). The highest stresses were limited to –40 MPa and the lowest, to –120 MPa. Areas No. 3, 7, 10 produced the humps and flat areas No. 1, 5, 9 – the dips in the stress distributions obtained. The stresses measured in the other bend areas had intermediate values. A reverse (cf. Fig. 7) decrease in the stress variation range was observed, with a certain positive trend in going from area No. 1 to area No. 11 (Fig. 8).

The study of intermediate cell No. 2 under external loading at P=50 N also demonstrated a tangible deviation from the cyclic distribution of stresses observed under no-load conditions. This difference manifests itself in correlating the layer-averaged stress values (see Fig. 8). Comparison of the figures suggests that all the flexures and flats are basically affected, causing an upward curve shift by 40-60 MPa, whereas the indents are practically unaffected.

Apart from the efforts discussed, some work was done to investigate hoop stresses in the spacer grid fixture fitted with the empty fuel rods mentioned above. The preliminary calculation results are in good agreement with the stress measurements.

CONCLUSION

An improved X-ray stress measurement procedure was used to study the distribution of residual stresses across the wall of fuel claddings and individual spacer grid cells and the distribution of operating stresses on the internal surface of spacer grid cells with empty fuel rods and exposed to external loading.

The studies on fuel claddings revealed the effect of the manufacturing process on the distribution of residual stresses and came up with recommendations on the process improvement.

The stress field produced by a given load was determined by analyzing the findings of spacer grid cell studies. The discovered characteristic cyclic distribution of circumferential cell stresses was attributed to the structural geometry of the cells: the extreme stress values were observed at indents and in flat areas of the cells. Stresses in the other flexed areas were found to have intermediate values.

The design of a special goniometric attachment was improved for staging oblique targeted X-ray diffraction measurements of stresses in selected areas inside spacer grid cells exposed to the action of inserted empty fuel rods and external loading.

The data obtained testified to a high sensitivity of the X-ray procedure in measuring stresses upwards of 10 MPa, which showed an average measurement error of ± 20 MPa in the value range from –300 MPa to +300 MPa with the confidence probability of 85%.

REFERENCES

1 Matsegorin I.V., Osipov V.V. Distribution of residual stresses in fuel claddings and spacer grids. Publishing House “Virazh Tsentr”, “*Izobretateli mashostroyeniyu”*, No. 2, 1997, p. 41.

2 Matsegorin I.V., Ablogin A.L., "Classification of textures of zirconium alloy products", "*Atomnaya Energy*", RU, Vol.65, publ.1, 1988, pp.38-42.

3 Matsegorin I.V., Rivkin E.U., Semenov A.N., Technique for an evaluation of anisotropy of mechanical properties of industrial items, 15th International Conference on Structural Mechanics in Reactor Technology, SMiRT-15, August 15-20, 1999, Seoul, Korea, L3-B5-RU.